Healthcare Analytics 4 (2023) 100253

Contents lists available at ScienceDirect

Healthcare Analytics

journal homepage: www.elsevier.com/locate/health

The visibility graph analysis of heart rate variability during chi meditation and Kundalini Yoga techniques

Mahda Nasrolahzadeh [a,*], Zeynab Mohammadpoory [b], Javad Haddadnia [a]

[a] Department of Biomedical Engineering, Hakim Sabzevari University, Sabzevar, Iran
[b] Department of Electrical Engineering, Shahrood University of Technology, Shahrood, Iran

ARTICLE INFO

Handling editor: Madijd Tavana

Keywords:
Visibility graph
Heart rate variability
Meditation
Nonlinear dynamics
Fractality
Complexity

ABSTRACT

The human heartbeat reflects one of the most crucial types of complex physiologic fluctuations. The purpose of this study is to study and evaluate the complexity of heart rate time series to capture its intrinsic multiscale dynamics based on the concept of fractality and complexity. The visibility graph (VG) of the heart rate series is proposed as a quantitative method to differentiate subjects in rest and meditation periods of two techniques: Chi meditation and Kundalini Yoga meditation. Differential complexities between the two mentioned states are quantified using the power of scale-freeness (PS) and the graph index complexity (GIC) in VG. The model is applied to available heart rate signals in the PhysioBank. The results reveal the promising ability of PS and GIC to assess the distinction between the two states. However, in both meditation techniques, the complexities of heart rate signals are increased during meditation. The results also show all heart rate series have visibility graphs with a power-law topology, and fractality in the heart rate series is dictated by a mechanism associated with the chaotic nature of the biological signals that could be useful to evaluate heart rate signals during meditation.

1. Introduction

Meditation is a technique which progressively used to deal with a variety of adverse conditions, embracing anxiety, chronic pain, and stress, based on a psychological intervention [1,2]. It aims at moderating the current thought by cutting the analytic burden and thwarting discursive and obsessive concepts [3]. Mindfulness meditation tries to have a great effect on the mind and body by using its two key principles, namely calm thinking and exercising self-control, leading to a significant reduction in anguish and stress. In addition, it affects diseases that are caused by stress, such as high blood pressure disorders, tension headaches, anxiety, and so on [4]. Hence, recent mindfulness meditation studies have focused on how to change the underlying mechanisms of practitioners' physiological conditions. For instance, Wallace found that oxygen consumption, skin resistance, heart rate, and specific electroencephalogram frequencies change during meditation [5]. Based on the fMRI monitoring, Phongsuphap et al. designed a study to find the functional relations between the pursuits of the autonomic nervous system (ANS) and meditation [6]. More specifically, meditation techniques have been investigated for heart rate variability analysis [7], endocrine system response detection [8], sleep studies [9], and mental disorders such as depression [10]. Despite manifold studies evaluating the possible health advantages of a variety of meditation techniques, clarifying the results of meditation practice and its underlying physiological mechanisms is still under research.

Recently, literature studies have focused on various aspects of the physiological system's effect on heart rate (HR) signals [11–13]. This focus is significant because much informative data is embedded in the HR time series. It has been shown that this data is directly related to human heart health. In addition, it can be helpful for diagnosing some cognitive pathologies of the central nervous system that cause heart disease. Moreover, describing the function of ANS branches in regulating the circulatory system by these signals has been recognized as an important non-invasive technique. It has also been found that heart coherence is forcefully associated with variability in HR and can be a suitable cardiac indicator for meditation states. In this regard, there are several studies investigating the variations in the dynamic behavior of the HR time series during meditation [14–16]. Initially, HR time series analysis was in terms of statistical indicators, but more complex analyzes were soon substituted to elicit more information from the signals. As an early method for analyzing HR series, largely spectral analysis is accepted. In this method, since it is the HR series, they are considered

* Corresponding author.
E-mail addresses: ms.nasrolahzadeh@yahoo.com (M. Nasrolahzadeh), z.mohammadpoory@gmail.com (Z. Mohammadpoory), Haddadnia@hsu.ac.ir (J. Haddadnia).

https://doi.org/10.1016/j.health.2023.100253
Received 7 December 2022; Received in revised form 8 April 2023; Accepted 31 August 2023
Available online 4 September 2023

with a great variety of various sources of noise. In addition, the analysis of non-stationary signals based on this method has been challenged. In the spectral analysis of some signals using traditional methods, there is typically a broad range of frequencies and false harmonics, most of which are eliminated. For instance, the Fourier spectral analysis process is associated with the super-linear positions of trigonometric functions in which the extra harmonic components present in most non-stationary biological signals, such as HR, lead to the production of disfigured wave profiles. These resulting disfigurements reflect nonlinear contributions. Hence, because the induction of false harmonic components occurs by non-stationary and nonlinear components in time series such as HR, traditional methods cannot be useful for their study [17,18].

The complexities of the behavioral and biological systems are a considerable challenge encountered in psychobehavioral research. In this context, it should be noted that some mathematical methods are capable of providing models for complex systems. Also, the dynamical behavior of bio-systems can be evaluated using nonlinear analysis [19, 20]. Since the dynamics of the cardiovascular system is non-stationary, complex, and chaotic, nonlinear approaches have been used to evaluate HR indices [21–23]. In recent years, several research studies have utilized nonlinear methods to quantitatively assess the effects of meditation on the behavior of biological time series, including electrocardiograms (ECG), electroencephalograms (EEG), and HR signals [24–26]. However, most available methods cannot adequately elicit the intricate details of HR signals. In addition, most available quantitative methods used to evaluate the dynamics of HR series assume stationarity of HR time series, in which the mean and variance of the signal do not change with time [19]. Although recent studies have drawn attention to the non-linear and non-stationary nature of the HR series, it limits the applicability of available methods for investigating complexity.

To investigate the fractality and complexity of signals, many new and powerful nonlinear approaches have recently been proposed that use both time series analysis and complex network theory. One of the simplest and most interesting methods proposed for representing the attributes of signals is the visibility graph (VG) method, which maps signals to graphs. It has been shown that VG can turn fractal signals into scaleless graphs [27]. In addition, it can use the scale-freeness degree for determining the fractality degree of the signals. Notably, it has been shown that various biological time series such as ECG [28], EEG [29], and speech [30] signals treat as processes with scale-invariant characteristics. For instance, Ahmadlou and Adeli presented the similarity of VG to estimate the complexity of dynamical systems associated with brain activities during autism neurodegenerative disorders [31]. Li et al. proposed a denoising approach called a weighted multi-scale limited penetrable visibility graph to detect the rhythms characterizing atrial fibrillation in noisy ECG signals [32]. Mohammadpoory et al. introduced a novel approach based on VG parameters for the automatic analysis of diabetic retinopathy phases [33]. They also presented weighted VG entropy for the diagnosis of seizures based on EEG signals and obtained a high diagnostic accuracy of 97% [34]. Nasrolahzadeh et al. constructed complex networks from HR time series during meditation and found that series with lengths of various epochs reveal different topological network structures [35]. In another study [36], to diagnose epileptic seizures in epileptic rats, some algorithms based on the VG method for converting electrocorticogram time series to graphs were proposed.

This research is designed to investigate and evaluate the complexity of the HR time series in describing the dynamics of its inherent multi-scale deal with the notion of fractality based on chaos and nonlinear theories. It aimed at identifying the performance of heart rate signals during two kinds of meditation (Kundalini Yoga meditation and Chi meditation) by utilizing VGs quantification analysis as descriptors of fractality (self-similarity) and complexity characteristics. It is also disputed that either complexity or fractality can present us with a better exposition of different psychological states (before and during meditation). Hence, in this study, the complexity of HRs is calculated using the VGs of HRs before and during meditation. In this spirit, the HR time series is mapped into a graph based on the maximum eigenvalue of the adjacency matrix and the power of scale-freeness (PS). Differential complexity between before and during meditation subjects are quantified using Graph index complexity (GIC). More specifically, this study is meant to answer the following question:

Can the two VG-based GIC and PS feature extracted from the HR signal provide a practical basis for detection in different psychological states (before, and during meditation) and in different meditation techniques?

The innovations of the paper are summarized as follows:

- VG of the HR signals is proposed as a quantitative method to differentiate subjects before and during meditation in two different meditation techniques.
- The power of scale freeness of VG is used to evaluate the fractality of HR signals during meditation.
- Differential complexities in two different states: before and during meditation are quantified using GIC.
- The weighted VG is also proposed for HR analysis for the first time.

The rest of this study is organized as follows: Section 2 briefly describes the utilized database and then the methods and applied quantification analysis. Section 3 presents the experimental results on the database. Section 4 deals with discussions. Finally, Section 5 states the conclusion of the paper and future works.

2. Material and methods

2.1. Database

In this paper, the Physionet database has been utilized to provide the HR signals of two groups of individuals doing Chi and Kundalini Yoga meditation correspondingly [37]. In what follows, these two techniques are described.

2.1.1. Chi meditation

A group of eight subjects, including three men and five women (26–35 years of age, mean 29 years), was purposefully selected to perform Chi meditation. All meditators were evaluated for general health before the start of the experiment. It was confirmed that they did not take any medication and did not suffer from heart disease or certain mental disorders. All of the meditators were graduate and postdoctoral students. They were also relatively beginners at meditation practice; most began their practice around one to three months before this study. The everyday activities of meditators, for about 10 h, were recorded while wearing a Holter recorder. The recording time took 5 h. After processing, it was found that each had done 1 h of meditation practice. During the practice task, the meditators silently listened to the master's instructions. Meditators were asked to visualize the opening and closing of a lotus in their stomachs while they breathed spontaneously. The session of meditation lasted about 1 h. After recording the HR signals, the necessary analyzes were made on them offline with a sampling rate of 360 Hz. The start and end times of meditation were determined separately by the symptoms of the event. Fig. 1 A&B depicts the HR signals captured from a subject before and during Chi meditation.

2.1.2. Kundalini Yoga meditation

A group of four subjects consisting of two women and two men (20–52 years of age, average 33 years) was considered for performing Kundalini Yoga. Meditators were at a high level of training. They were asked to wear a Holter monitor for about an hour and a half. Initially, the baseline calm breathing lasted 15 min, and then 1 h of meditation was recorded. This type of meditation consisted of breathing exercises and chanting performed in a sitting position with crossed legs. The start and end of meditation stages were signed with the event symptoms. The sampling rate was considered 360 Hz. The HR signals belonging to a

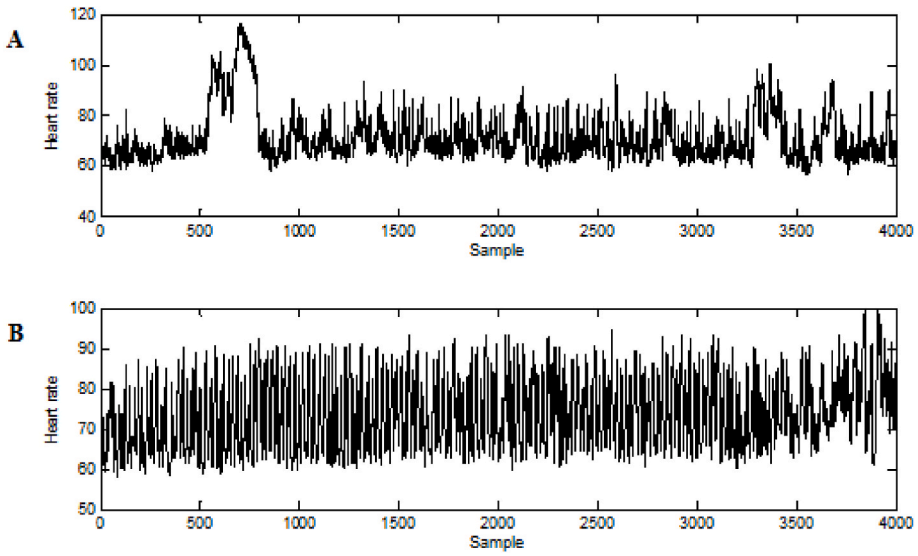

Fig. 1. Heart rate time series from a subject (A) before meditation and (B) during Chi meditation.

subject before and during Kundalini Yoga meditation are shown in Fig. 2 A&B.

2.2. Data augmentation

Data augmentation can be considered an important preprocessing step, especially where large training data are required for analysis. Several techniques such as window slicing and window warping have been introduced to augment time series data [38]. In this study, the method introduced by Deka and Deka was used [11]. In the presented method, first, the original signal is connected with its duplicate version at the end. Then, from this concatenated signal, eight excerpts of 5 min are extracted by a sliding window. In this method, the length of the original signal should be considered longer than the length of the excerpt. Also, extracting excerpts with a length less than the actual signal, confirms that enough parts of the data points in all the excerpts are unique to each other. As shown in Fig. 3, the original signal is spliced at the end of the signal with duration of 8.7 min. By duplicating itself, it produces a signal with duration of 17.4 min. Now, if the window (size 5 min) is moved from its zero position by 2 min, a sample is obtained that starts at 2 min and continues to 7 min.

This generated excerpt will have the same data points as those at 2–5 min and then 0–2 min of data from the original signal. However, in our case, the generated excerpt captures data points from 2 to 7 min of the original signal, i.e., the length of the original signal is 8.7 min. Therefore, provided that the length of the excerpts is shorter than the original version, the mentioned method can better solve the problem of data redundancy. Finally, the amount of window displacement is calculated with the aim of avoiding the possibility of maximum overlap between two consecutive excerpts. The following equation calculates the appropriate window shift [11]:

$$T_N + (T_W - 0.1T_N) = T_W + N(M-1) \;\; \& \;\; 0.9T_N = 7N \tag{1}$$

where T_W and T_N denote the time durations of the window and the original signal to be augmented, respectively. Moreover, N is the number of shifts that could be made. Note that, M denotes the number of segments to be obtained, which in this study yielded 8 for Kundalini Yoga and 35 for chi meditation signals.

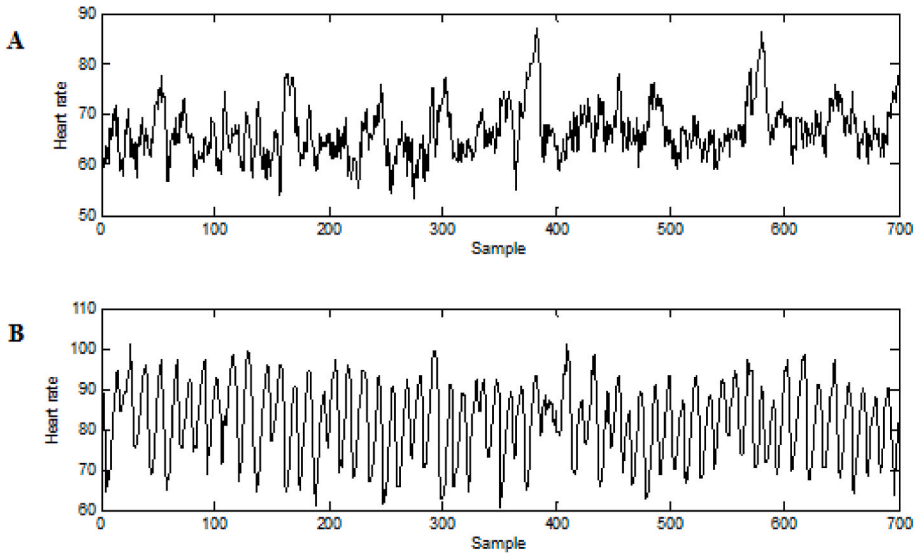

Fig. 2. Heart rate time series from a subject (A) before meditation and (B) during Kundalini Yoga meditation.

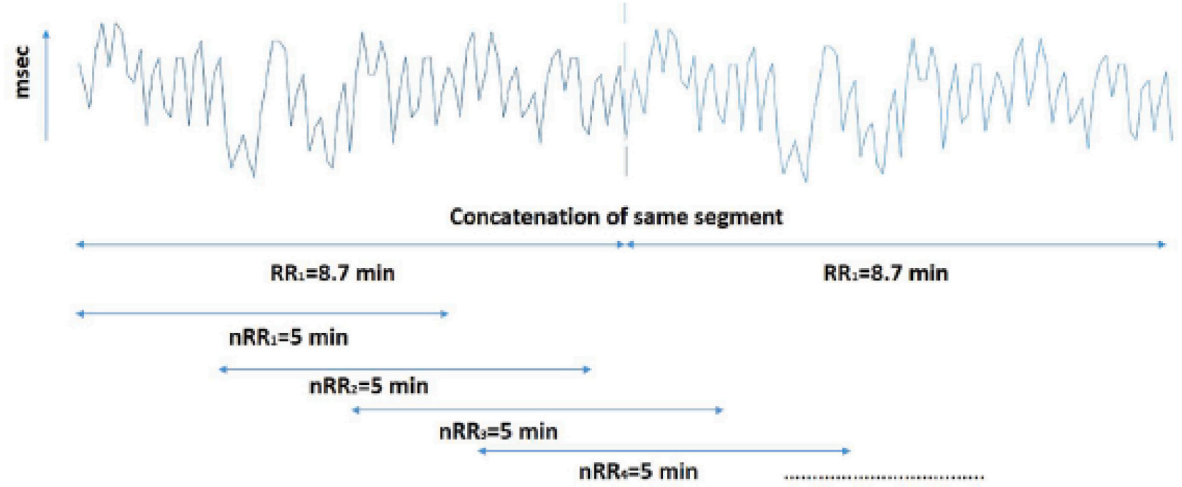

Fig. 3. An example of data augmentation based on concatenation and sliding window of width 5 min [11].

2.3. VG

One of the most attractive approaches which have recently interested extensive attention is the VG algorithm, converting time series into the demonstrations of a complex network [27,39]. In essence, the theory used in this algorithm is based on the analysis of the reciprocal visibility relations between points and barriers in two-dimensional sceneries in terms of calculative geometry, which is introduced for ECGs and other biological time series with applications ranging. This is mainly because the visibility algorithm forms a set of geometric and sequential criteria for time series with the real scalar value that results in a combined demonstration of the underlying dynamic system.

In VG algorithm theory, each graph node represents an example of a signal. Connecting the corresponding nodes means that the two samples can sight each other [39]. To see this, suppose Y_i is the i th point of the signals. Accordingly, as shown in Fig. 4, there is a connection of two nodes, Y_a and Y_b, to each other by an edge, and they can sight one another if and only if:

$$Y_{a+i} < Y_b + \left[\frac{b-(a+i)}{b-a}\right].(Y_a - Y_b), i \in Z^+, i < (b-a) \quad (2)$$

According to this algorithm, each example of the signal, which is each point in the HR time series, denotes a node in the graph. When two instances see each other, it leads to the connection of the corresponding nodes (Fig. 4 and Eq. (2)). Fig. 4 illustrates how the time series data (Fig. 4A) is mapped to its VG (Fig. 4B). Notably, in Fig. 4A, the green line connects the two instances that are capable of sighting each other. The curved lines connect the vertices of the VG through a two-sided edge, as shown in Fig. 4B. The resulting VG structure may be unfolded some hidden dynamical properties like complexity and similarity in the time-series signal.

A weighted visibility graph (WVG) was introduced by Supriya et al. [40]. They showed that in this algorithm, the link weight varies with the fluctuation of EEG signal values, therefore facilitating the discrimination

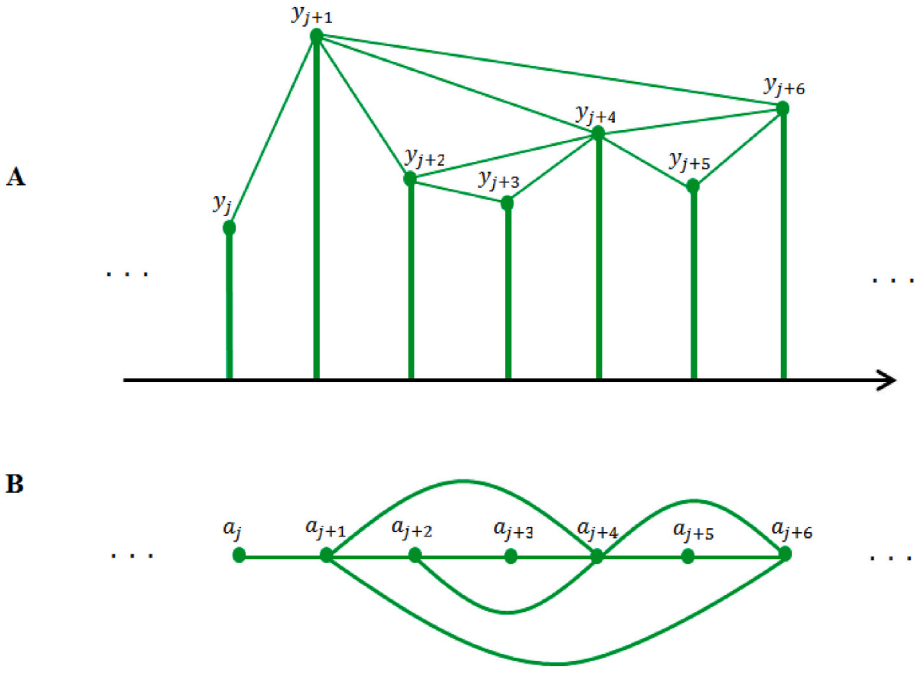

Fig. 4. An example of converting an HR time series to its VG. The upper part (A) represents an HR time series $\{y_j\}$ with 7 instances. The bottom part (B) shows the VG elicited from its time series with node sequence $\{a_j\}$.

of various EEG signals. The weight w_{ij} of edge e_{ij} between nodes n_i and n_j can be calculated as follows:

$$c = \begin{cases} \arctan\left(\dfrac{x(t_j) - x(t_i)}{t_j - t_i}\right) i < j \quad e_{ij}\ exists \\ 0 \quad otherwise \end{cases} \tag{3}$$

2.4. Complexity of VG

Estimating the complexity of VG can obtain the fractality (self-similarity) and complexity associated with a time series simply and similarly to calculating fractal dimension (FD), with the advantage that there is no need to make the state space where a large number of data points are required [39]. In what follows, two methods are addressed for measuring complexity based on VG.

2.4.1. PS based VG

The obtained VG from a periodic signal in which all nodes are connected to the number of edges alike, appearing as a fractal time series mapped into a graph with a structural scale-free known as the power law as follows:

$$P(k) = k^{-\alpha} \tag{4}$$

where k denotes the number of edges linked to a node, namely, the sequence of a node. Besides, P represents the probability distribution of the edges, connecting to the vertices of a graph. Furthermore, α refers to the power of scale-freeness (PS) in VG.

Note that calculating the power of the free-scale structure of the VG as the slope of $log_{10}[P(K)]$ versus $log_{10}\left(\frac{1}{K}\right)$ is associated with the quantities of complexity and fractality of the time series. Notice also that one of the manifestations of disorder and chaos is fractal geometry, and the FD can quantify the fractality of time series. Therefore, the slope of $P(k)$ vs. $\frac{1}{k}$ in a log–log plane suggests the FD of the signal [31,41]. The steps of the PS-based VG algorithm are presented in Algorithm 1.

Algorithm 1
Pseudo-code for extracting PS-based VG algorithm

```
Input: Y: Heart rate time series
  Output: Extracted PS using Eq. (4)
    Calculate size Y
    for i = 1 : size(Y, 1) do
    Generate adjacency matrix A based on size Y
      Adjust so that minimum of Y is at zeroY = Y− min(Y)
      for i = 1 : N − 1 do
      Compute all subsequent gradients
        Compute vector of as δY
          Compute time from current reference i as δ
        Compute total gradientsm = δY./δ
          for j = 1 : N − i do
            cummax(j) = max(m(1 : j))
          end for
            links = (m >= cummax)
            A(i, i + 1 : end) = links
  end for
  Compute the degree distribution
    k = sum(A)
      k = full(k)
      dk = zeros(1, length(k))
  end for
```

2.4.2. GIC based VG

GIC is another measure that can extract informative properties from the structure of time series based on the complexity of a graph [42].

Consider a graph with k nodes that owns an adjacency matrix to the largest eigenvalue, λ_{max}, for the weighted or unweighted graph. Hence, this measure can be described as follows [43]:

$$C_{\lambda_{max}} = 4c(1 - c) \tag{5}$$

where

$$c = \frac{\lambda_{max} - 2\cos(\pi/(k+1))}{k - 1 - 2\cos(\pi/(k+1))} \tag{6}$$

Notably, $C_{\lambda_{max}}$ alters between zero and one for all of the graphs with both unweighted and bidirectional properties. It is because of holding the following inequality for them.

$$2\cos\left(\frac{\pi}{k+1}\right) \le \lambda_{max} \le k - 1 \tag{7}$$

In addition, the larger value of $C_{\lambda_{max}}$ indicates that the graph has a more complex structure. The steps of the GIC-based VG algorithm are presented in Algorithm 2.

Algorithm 2
Pseudo-code for extracting GIC-based VG algorithm

```
Input: Y: Heart rate time series
  Output: Extracted GIC using Eq. (5)
  Calculate size Y
    Generate adjacency matrix A based on size Y
      Adjust so that minimum of Y is at zero
      Compute all subsequent gradients using Eq. (6)
        for i = 1 : N − 1 do
      Compute all subsequent gradients
        Compute vector of deltay's
        Compute time from current reference i
        for j = 1 : N − i
        cummax(j) = max(m(1 : j))
        end for
        links = (m >= cummax)
    end for Stop the loop and product O_j
  Store this information in the adjacency matrix, A
      A(i, i + 1 : end) = links
  end for
```

3. Experimental results

Because visualization can facilitate pattern recognition and allow the user to see patterns [44], VG plots were drawn from the HR time series. Fig. 5A-D illustrates VG plots of 100 data samples of the series of HRs for Chi and Kundalini Yoga meditation techniques in two different states: during and before meditation.

As shown in Fig. 5, an increase in the number of links in VGs for subjects during meditation compared to pre-meditation is evident in both techniques. This presents an increase in the complexity of the behavior of the HR signals during meditation. It should be noted that the black lines drawn in Fig. 5 show the relative changes in VG complexity. In addition, the red dots as VG nodes correspond to the quantities of the data samples in the time series, making them visible to plenty of other data samples, leading to their corresponding nodes being hubs of the visibility graph. Fig. 6A-D depicts the WVG of the series of HRs for Chi and Kundalini Yoga meditation techniques in two different states: during and before meditation.

These plots display that the estimated VGs are different for the two mentioned techniques in two different states (before and after meditation). Consequently, it is evident that the dynamics of the HR signals are completely different before and during meditation. Hence, in what follows, the dynamical behaviors of the time series of subjects' heart rates during and before meditation will be further investigated more elaborately using this characteristic based on complexity and fractality. The motivation for this effort is to find out if it can be used to measure the physiological impact on individuals practicing meditation techniques.

To do this, the effectiveness of the VG has been demonstrated by developing PS (case study-I) and GIC (case study-II) analyses for HR time series in two different states, namely, Chi and Kundalini Yoga meditation techniques.

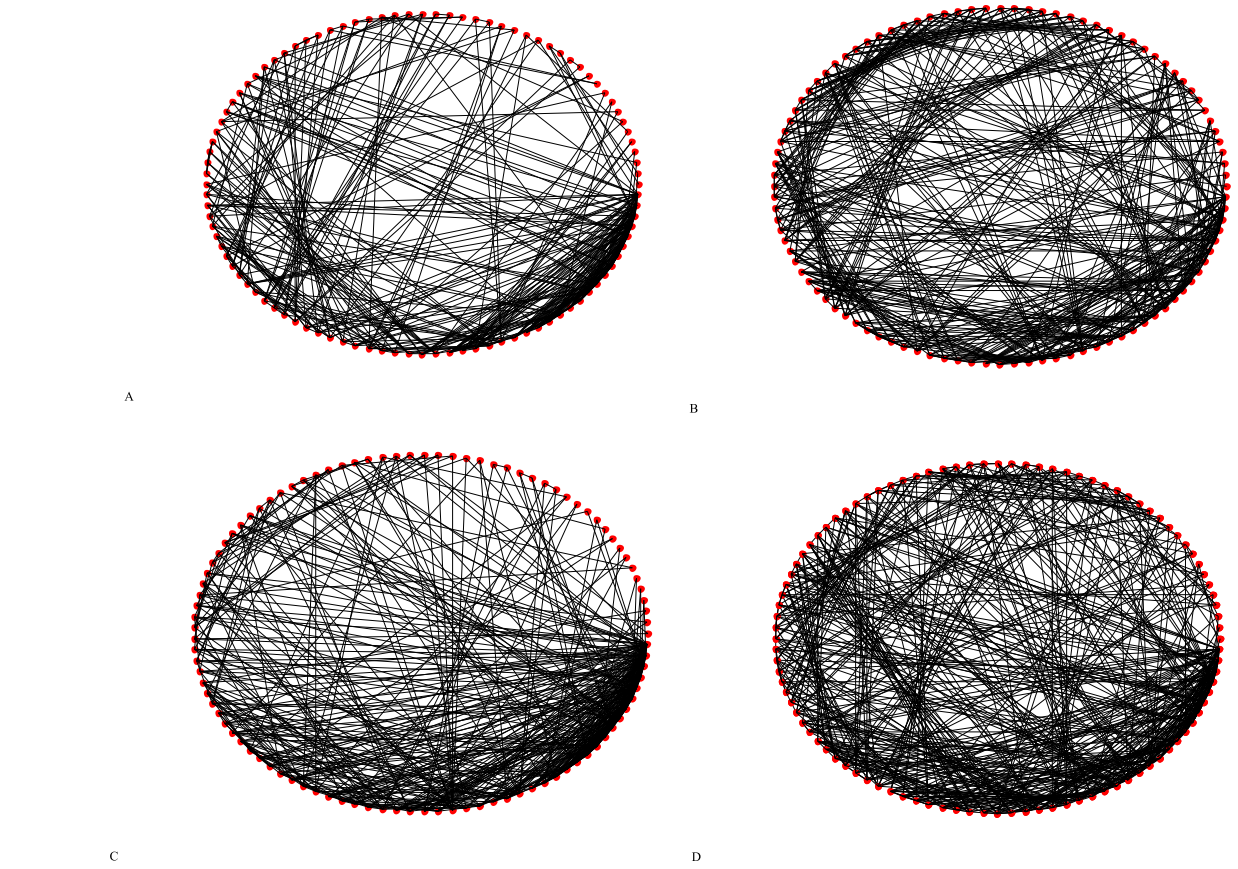

Fig. 5. Representative VG with 100 data samples of the heart rate signals (A) before meditation, (B) during meditation belonging to the Chi technique from record C1 as well as (C) before meditation, and (D) during meditation belonging to the Kundalini Yoga technique from record Y8.

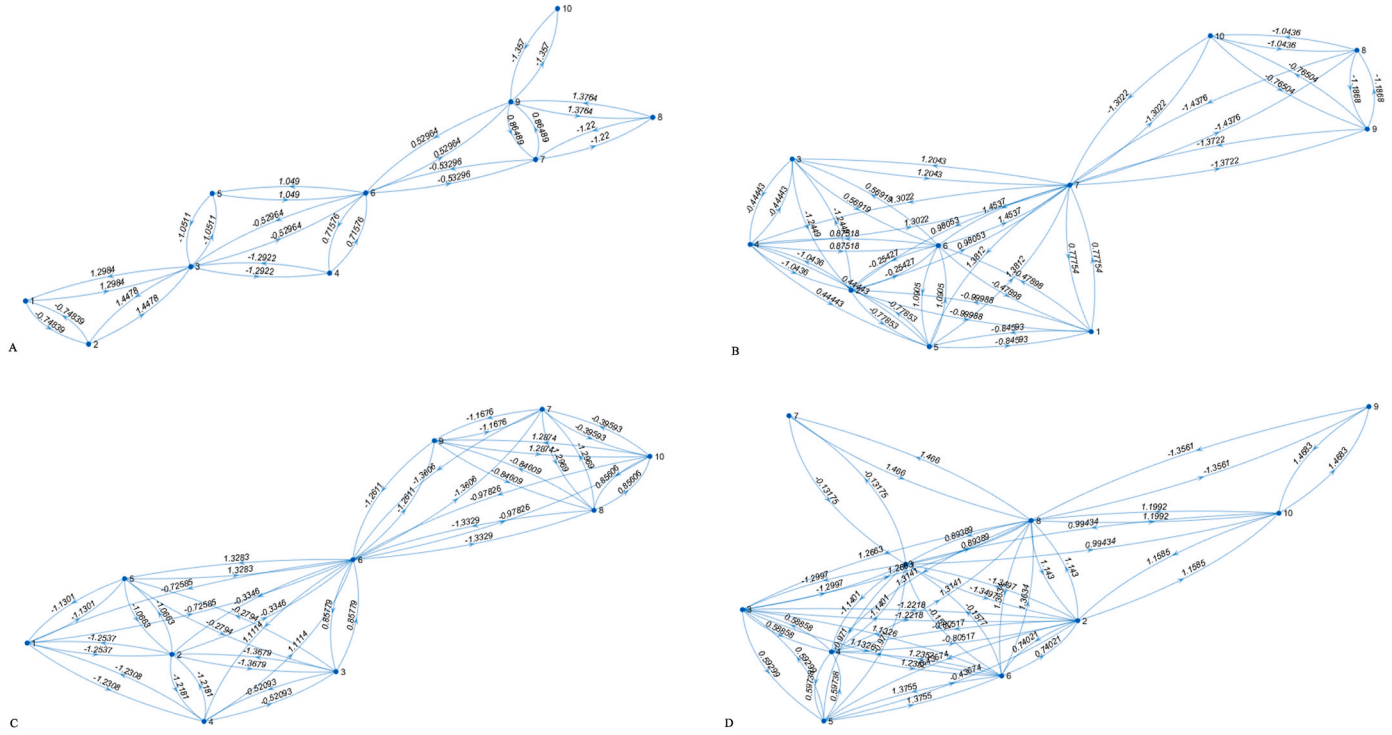

Fig. 6. Representative edge-weighted in the graph based on the adjacency matrix of the heart rate signals (A) before meditation, and (B) during meditation belonging to the Chi technique from record C1 as well as (C) before meditation, and (D) during meditation belonging to the Kundalini Yoga technique from record Y4.

3.1. Case study-I: analysis of the HR time series based on PS

To quantitatively scrutinize the HR time series based on the PS parameter, the quantities of P(K) vs. K were calculated for all constructed VGs to yield the slope value dealing with the fractality of the signal. On this note, time series were first windowed using non-overlapped rectangular windows. Two epoch lengths were used for the analysis: 500 samples and all samples in each time series. The number of 500 samples was sufficient for analysis, but since the number of all samples for analysis was small, the data from both techniques were augmented. Then, power-law conduct was determined according to P(K) versus 1/K for each HR time series. Finally, the PS parameter in terms of the slope of the $\log_{10}[P(K)]$ against $\log_{10}(\frac{1}{K})$ was calculated for HR signals before and during meditation of both mentioned techniques. Note that, the computational time for calculating this parameter was 11.055 s. Figs. 7 and 8 illustrate the cumulative degree distributions, P(K), out of the heart rate series of individuals with 500 sample epochs in two different states: pre-and during Chi and Kundalini Yoga meditation techniques. In addition, the P(K) of the VG of HR series with all augmented data samples for before and during two forms of meditation are shown in Figs. 9 and 10. These figures depict the fractality of the signals on the log-log plane based on the slope of P(K) vs. $\frac{1}{K}$. Because there was the topology of the power law with increasing K for two techniques in two different states: pre-and during meditation, calculating the slope value was made using the least squares (LS) fit procedure in this study. The extracted PS for two types of meditation showed considerable discrimination (p-value = 0.05) between before and during meditation with 500 sample epochs and all data samples.

From the figures, it was obvious that the values of PS based on 500 sample epochs were calculated as 1.98 for before and 3 for during Chi meditation. Moreover, they were calculated as 1.78 for before and 2.95 for during Kundalini Yoga meditation. Besides, the values of PS based on all augmented data samples were calculated as 1.44 for before and 1.64 for during Chi meditation. In contrast, they were calculated as 2.03 for before and 2.79 for during Kundalini Yoga meditation. Therefore, these depict that the PS of the signal is increased during meditation. Moreover, there is a power-law topology with increasing k in two groups (before, and during meditation) and in different meditation techniques.

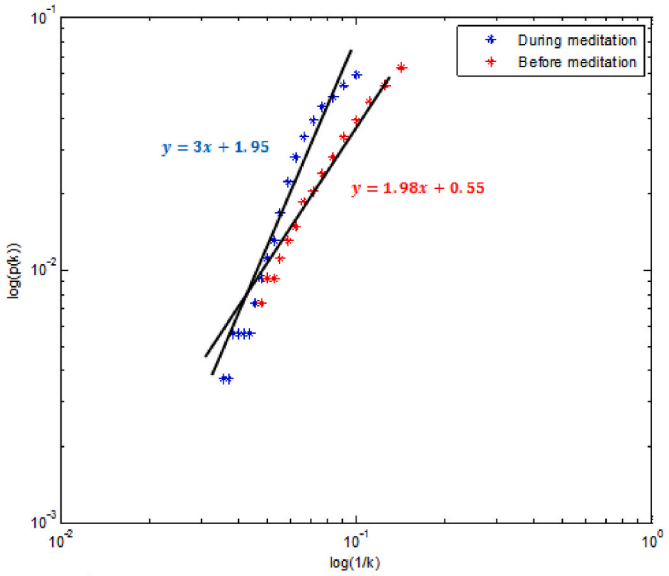

Fig. 7. Log-Log $P(K)$ vs. $\frac{1}{K}$ of the VGs with 500 sample epochs for the heart rate series of subjects: pre-and during Chi meditation. The black line represents the fitted line to the samples via the LS method.

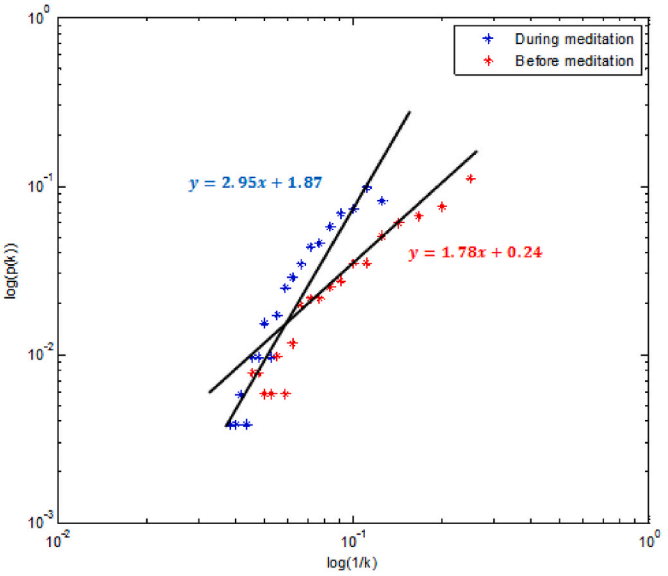

Fig. 8. Log-Log $P(K)$ vs. $\frac{1}{K}$ of the VGs with 500 sample epochs for the heart rate series of subjects: pre-and during Kundalini Yoga meditation. The black line represents the fitted line to the samples via the LS method.

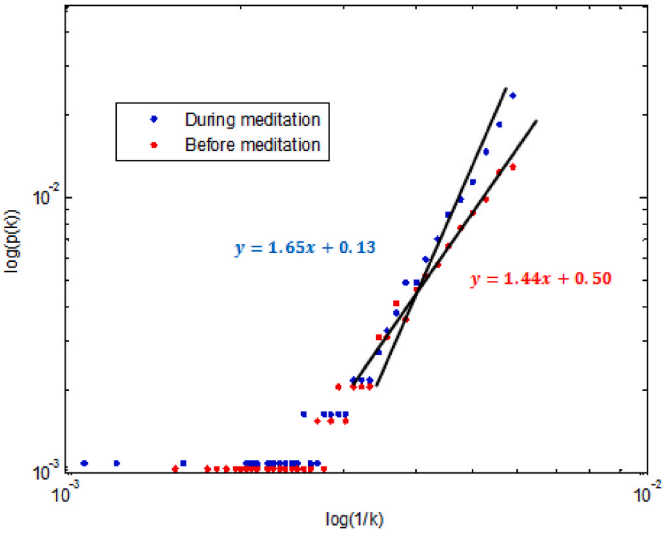

Fig. 9. Log-Log $P(K)$ vs. $\frac{1}{K}$ of the VGs with all augmented data samples for the heart rate series of subjects: pre-and during Chi meditation. The black line represents the fitted line to the samples via the LS method.

3.2. Case study-II: analysis of the HR time series based on GIC

It was needed to segment heart rate signals for quantification analysis of the complexity of the heart rate signal based on the GIC parameter to be performed. Hence, the HR signals were windowed by non-overlapped rectangular windows. The length of the epochs was considered to be 500 data samples and all augmented data samples for analysis. The data were augmented based on the technique described in section 2.2. Then, the GIC values were calculated by converting these epochs to unweighted and weighted VGs. The computational time for GIC estimation based on unweighted and weighted VGs was 13.425 and 12.351 s, respectively.

3.2.1. Analysis of GIC based on unweighted VG

In this regard, to demonstrate the effectiveness of the proposed method, the values of the average and standard deviation of GIC based

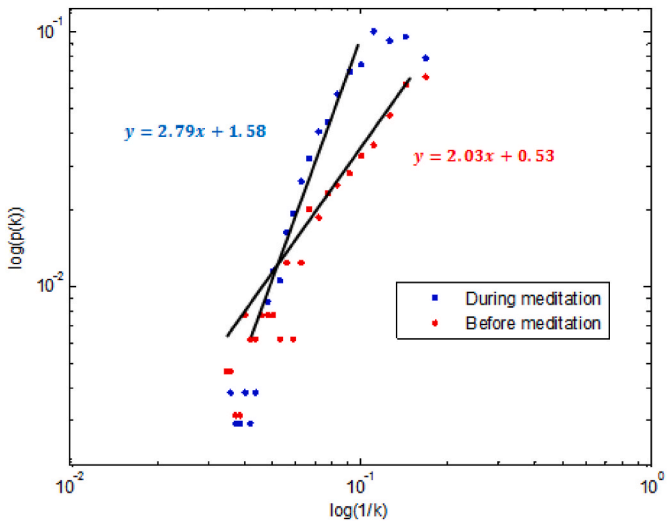

Fig. 10. Log-Log $P(K)$ vs. $\frac{1}{K}$ of the VGs with all augmented data samples for the heart rate series of subjects: pre-and during Kundalini Yoga meditation. The black line represents the fitted line to the samples via the LS method.

on unweighted VG for subjects with 500 and all augmented data samples in two different states: before and during two meditation techniques, are provided in Tables 1 and 2. The results show that subjects during meditation have notably higher GIC values for the HR signals than subjects before meditation. This means that the complexity of the HR time series increases during meditation.

The one-way analysis of variance (ANOVA) test, as the statistical analysis, was fulfilled to specify the ability of GIC based on unweighted VG to differentiate the HR signals of subjects before and during two meditation techniques. Notably, this test produces a number known as the P-value for evaluating the discrimination ability of the feature. It changes between 0 and 1, so when the P-value approach 1, suggesting the closeness and similarity of the distribution of groups, and when the P-value approach 0, suggesting the great suitability of the feature to distinguish groups. Tables 3 and 4 show the results of the ANOVA test with 500 sample epochs based on unweighted VG in different states of the two meditation techniques.

Moreover, Tables 5 and 6 show the results of the ANOVA test with all augmented data samples in different states of the two meditation techniques.

Considering a threshold p-value of 0.05, a significant difference exists between the GIC based on unweighted VG of the HR series of the two groups according to the ANOVA results. This finding points to the fact that by increasing the GIC values, the complexity, and chaos of the dynamic behavior of the HR during meditation increases. Figs. 11 and 12 show the box plot of GIC values based on unweighted VG with 500 sample epochs in two different techniques, before and during meditation, respectively.

Furthermore, Figs. 13 and 14 show the box plot of GIC values based on unweighted VG with all augmented data samples for the two mentioned techniques, before and during meditation, respectively.

3.2.2. Analysis of GIC based on weighted VG

To further investigate the robustness of the proposed method, an experimental study was conducted on 500 samples and all augmented data samples of both Chi and Kundalini Yoga meditation. Then, GIC values based on WVG were calculated. Tables 7 and 8 show the average and standard deviation of GIC for subjects with 500 and all augmented data samples in two different states: before and during two meditation techniques.

Tables 9 and 10 show the results of the ANOVA test with 500 sample epochs based on WVG in different states of the two meditation techniques.

Moreover, Tables 11 and 12 show the results of the ANOVA test with all data samples in different states of the two meditation techniques.

Figs. 15 and 16 show the box plot of GIC values with 500 sample epochs based on WVG for the two mentioned techniques, before and during meditation, respectively.

Figs. 17 and 18 show the box plot of GIC values with all augmented data for the two mentioned techniques, before and during meditation, respectively.

Since GIC deals with the complexities of the time series of signals, it

Table 1
GIC results with 500 sample epochs based on unweighted VG for two meditation techniques: before vs. during meditation.

GIC (Mean ± Standard deviation)	before meditation	during meditation
Chi meditation	0.1208 ± 0.0175	0.1613 ± 0.0190
Kundalini Yoga meditation	0.1157 ± 0.0244	0.1604 ± 0.0123

Table 2
GIC results with all augmented data samples based on unweighted VG for two meditation techniques: before vs. during meditation.

GIC (Mean ± Standard deviation)	before meditation	during meditation
Chi meditation	0.0259 ± 0.0065	0.0369 ± 0.0033
Kundalini Yoga meditation	0.0629 ± 0.0329	0.1089 ± 0.0059

Table 3
ANOVA test results with 500 point epochs based on unweighted VG: before vs. during Chi meditation.

ANOVA					
Source of variation	ss	df	MS	F	Prob > F (P-value)
Between group	0.05358	1	0.05358	157.12	4.02326 e^{-24}
Within group	0.04433	130	0.00034		
Total	0.09791	131			

Table 4
ANOVA test results with 500 point epochs based on unweighted VG: before vs. during Kundalini Yoga meditation.

ANOVA					
Source of variation	ss	df	MS	F	P-value
Between group	0.00518	1	0.00518	15.55	0.0076
Within group	0.002	6	0.00033		
Total	0.00718	7			

Table 5
ANOVA test results with all augmented data samples based on unweighted VG: before vs. during Chi meditation.

ANOVA					
Source of variation	ss	df	MS	F	Prob > F (P-value)
Between group	0.00048	1	0.00048	18.07	0.0008
Within group	0.00037	14	0.00003		
Total	0.00086	15			

Table 6
ANOVA test results with all augmented data samples based on unweighted VG: before vs. during Kundalini Yoga meditation.

ANOVA					
Source of variation	ss	df	MS	F	P-value
Between group	0.00423	1	0.00423	7.59	0.0331
Within group	0.00334	6	0.00056		
Total	0.00758	7			

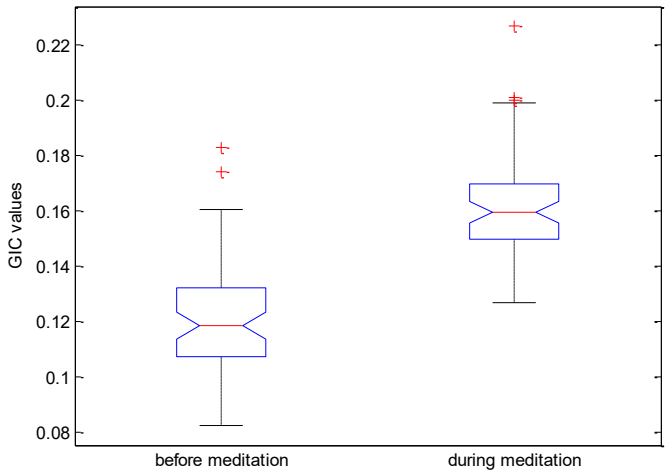

Fig. 11. Box plot of GIC values based on unweighted VG with 500 sample epochs belonging to all subjects before vs. during Chi meditation.

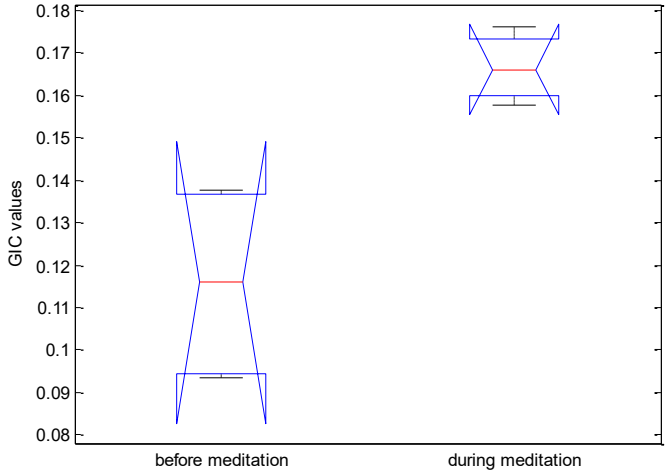

Fig. 12. Box plot of GIC values based on unweighted VG with 500 sample epochs belonging to all subjects before vs. during Kundalini Yoga meditation.

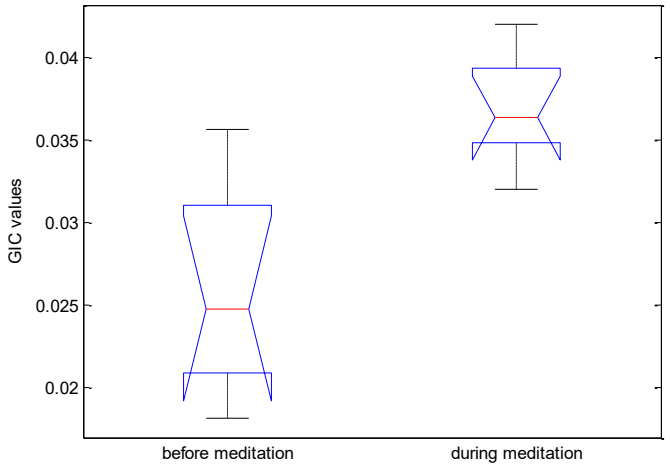

Fig. 13. Box plot of GIC values based on unweighted VG with all augmented data samples belonging to all subjects before vs. during Chi meditation.

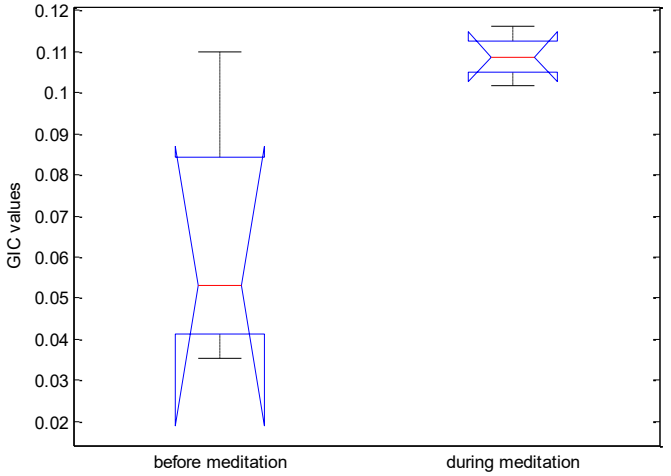

Fig. 14. Box plot of GIC values based on unweighted VG with all augmented data samples belonging to all subjects before vs. during Kundalini Yoga meditation.

Table 7
GIC based on WVG results with 500 sample epochs for two meditation techniques: before vs. during meditation.

GIC (Mean ± Standard deviation)	before meditation	during meditation
Chi meditation	0.1895 ± 0.0366	0.2755 ± 0.0124
Kundalini Yoga meditation	0.1882 ± 0.0293	0.2318 ± 0.0147

Table 8
GIC based on WVG results with all augmented data for two meditation techniques: before vs. during meditation.

GIC (Mean ± Standard deviation)	before meditation	during meditation
Chi meditation	0.0542 ± 0.0029	0.0665 ± 0.0042
Kundalini Yoga meditation	0.0884 ± 0.0274	0.1098 ± 0.0147

Table 9
ANOVA test results with 500 sample epochs based on WVG: before vs. during Chi meditation.

ANOVA					
Source of variation	ss	df	MS	F	Prob > F (P-value)
Between group	0.38468	1	0.38468	12.81	0.0004
Within group	8.17084	272	0.03004		
Total	8.55553	273			

Table 10
ANOVA test results with 500 sample epochs based on WVG: before vs. during Kundalini Yoga meditation.

ANOVA					
Source of variation	ss	df	MS	F	P-value
Between group	0.08235	1	0.08235	10.13	0.0079
Within group	0.09758	12	0.00813		
Total	0.17993	13			

is inferred that the complexity of the HR signals of subjects during meditation is more than before meditation. This evidence endorses using a nonlinear feature called the Hurst exponent to determine differential complexities in two different states, before and during meditation [14].

Notably, the data for Kundalini yoga was less than that for Chi meditation. In other words, the HR signals of the two meditation techniques had different sample sizes for analysis. However, according to the

Table 11
ANOVA test results with augmented data: before vs. during Chi meditation.

ANOVA					
Source of variation	ss	df	MS	F	Prob > F (P-value)
Between group	0.00481	1	0.00481	379.02	8.45213e-40
Within group	0.0016	126	0.00001		
Total	0.00641	127			

Table 12
ANOVA test results with augmented data: before vs. during Kundalini Yoga meditation.

ANOVA					
Source of variation	ss	df	MS	F	P-value
Between group	0.00733	1	0.00733	15.14	0.0002
Within group	0.03002	62	0.00048		
Total	0.03736	63			

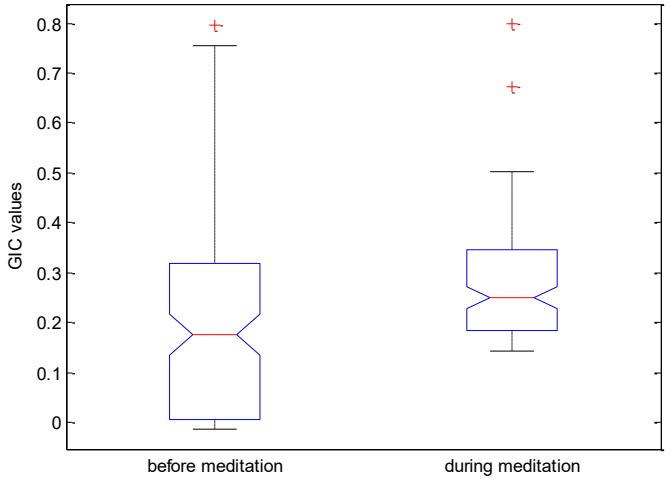

Fig. 15. Box plot of GIC values based on WVG with 500 sample epochs belonging to all subjects before vs. during Chi meditation.

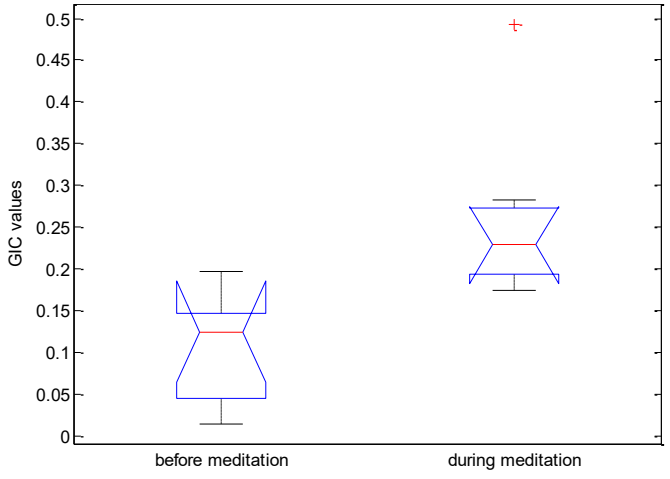

Fig. 16. Box plot of GIC values based on WVG with 500 sample epochs belonging to all subjects before vs. during Kundalini Yoga meditation.

results, compared with pre-meditation, the complexity of HR oscillations increased during the two types of meditation. The results indicate that VG analysis is not dependent on the sample size of the time series. It can deliver reliable and powerful results even if the time series be very short.

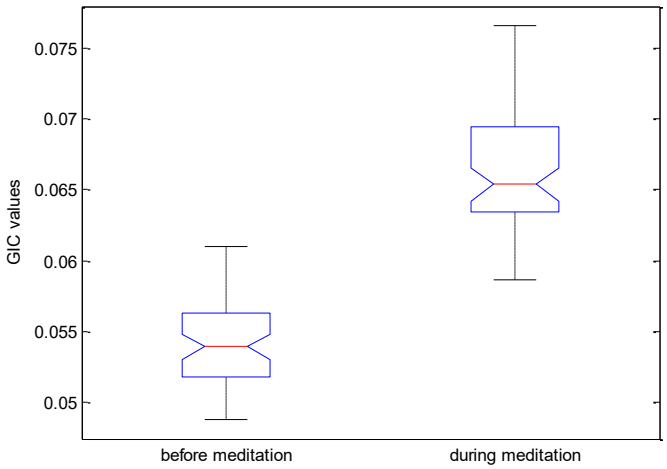

Fig. 17. Box plot of GIC values based on WVG with augmented data belonging to all subjects before vs. during Chi meditation.

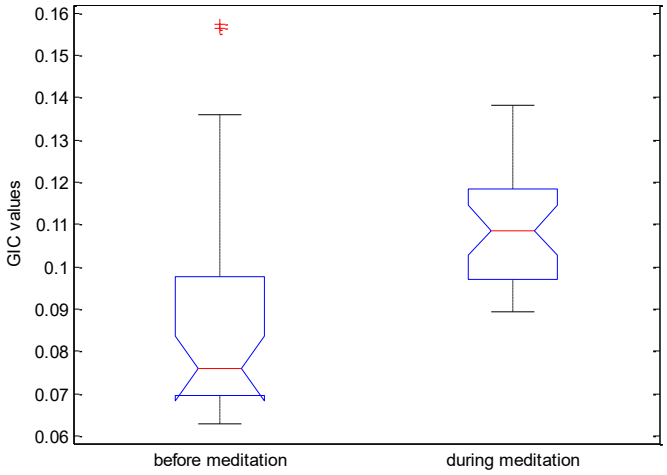

Fig. 18. Box plot of GIC values based on WVG with augmented data belonging to all subjects before vs. during Kundalini Yoga meditation.

4. Discussion

The present study was directed toward examining the large-scale dynamics of heart rate signals in particular psychophysiological states. It aimed at identifying the performance of heart rate signals during two kinds of meditation (Kundalini Yoga meditation and Chi meditation) by utilizing VGs quantification analysis as descriptors of fractality (self-similarity) and complexity characteristics. To do this, the VG algorithm was employed to estimate the fractality and complexity of the HR time series. Then, these characteristics were quantified from the HR time series using PS in various scales (Case study-I) and GIC (Case study-II). In this way, the dynamics of large-scale heart rate oscillations of the physiological system during two types of meditation were investigated. All the HR signals demonstrate a power-law topology as a measure of fractality and complexity. It supported that the nature of HR signals owns fractal and non-stationary for subjects during and before meditation.

The lengths of the time series analyzed were different in the two meditation techniques, as described in section 3. Therefore, in this study, it was evaluated whether the length of the time series can affect the results. To see this, HR time series were analyzed based on two epoch lengths utilizing the VG method. At first, VG was made of lengths with

500 samples, and then all augmented samples were applied for VG construction in each time series. The results show that for the lengths with 500 samples, the GIC values are increased during meditation for the two meditation techniques. Moreover, the increased complexity of heart rate and P-values during meditation indicated significant effects of meditation on GIC values (Tables 3 and 4). Besides, the results showed that the obtained GIC values where each time series was analyzed with all augmented samples increased for all individuals during meditation (Tables 5 and 6). The results in Tables 1 and 2 suggest that the GIC values are not very different for 500 sample epochs compared to those for all augmented samples. Furthermore, the PS values were visibly distinct from each other in two before and during meditation states. Besides, the PS parameter was shifted to higher values during meditation in both techniques. The results show that the GIC values based on unweighted and weighted VGs are increased during meditation for the two meditation techniques. Moreover, the increased complexity of heart rate and P-values during meditation indicated significant effects of meditation on GIC values. These findings reveal the fact that VG analysis has no prerequisites for the sample size to be large. On the other hand, the results also show that this theory can provide credible results with less than 500 data samples. This finding is supported by studies that have analyzed cardiac dynamics based on multi-fractal methods [45, 46].

Notably, previous studies have shown correlations of long-range power law in an extensive domain of complex physiological systems like neurons of medullary sympathetic in neural physiology [47] and heart rate [28], which reflects the fractal dynamic behavior of such biological systems. Hence, the loss of such dynamism and chaos causes unusual functions, including congestive heart failure, seizures, and other disorders. For instance, Adeli et al. reported that there are lower values of chaos and complexity in EEG signals of epileptic seizures in comparison with the normal state [48]. Bhaduri et al. found that the chaos and complexity of HR signals in congestive heart failures are lower than in a healthy state [49]. In addition, it is widely reported that meditation improves body function and is effective in correcting mental disorders and health issues [50–52].

Furthermore, a brief comparison between our proposed approach and other studies developed recently is represented in Table 13. We have tried to evaluate those works that had common objectives with our work. Notably, a precise comparison of the studies is a difficult task since different researchers have employed diverse methods for realizing the biomedical influences of various meditation techniques. Moreover, the number of HRs recorded for different techniques is unbalanced. Besides, most performance benchmarks are not reported.

All in all, the difference in response rates between before meditation and during meditation confirms that a remarkable group difference exists between individuals in the two mentioned states and in the two meditation techniques. Therefore, these differences indicate that the two seemingly different meditation protocols lead to some significant physiological responses.

The findings of the present study suggest that the analysis of heart rate signals based on VGs can reveal features containing useful information. Furthermore, the proposed method allows for acquiring profound insights into the organization of cardiac signals in various psychological conditions (pre and during meditation) by exploring the features offered by visibility graph theory.

5. Conclusion

This paper presented an experimental study of the effectiveness of utilizing the VG algorithm to quantify fractality and complexity as long-range correlations of HR signals. HR time series based on GIC and PS parameters for the pre-meditation state were compared with those during meditation in different meditation techniques. The results show the favorable capability of the GIC to evaluate the dynamical behavior of the HR time series during meditation. The GIC values during meditation are higher than before meditation, confirming the evidence that meditation influences heart rate dynamics and, to be precise, increases the degree of complexity. It is also revealed that the VGs in each of the HR series display fractality and power-law topology, which hint at the significant impacts of meditation techniques. In a nutshell, VGs, as a nonlinear method that captures informative data about the behavior of a dynamical system, can be successfully used to d distinguish between diverse states of heart rate variability in different psychological

Table 13
Comparison of the proposed method with other studies.

Reference	Meditation	Methods	Performance evaluation	Result
Zeng et al. [53]	Chi and Kundalini Yoga	Empirical mode decomposition based power difference	Student's t-test	$p < 0.01$ for Chi $p < 0.05$ for Kundalini
Li et al. [15]	Chi and Kundalini Yoga	base-scale entropy	*t*-test	BSEn decreases ($p < 0.05$)
Raghavendra and Dutt [54]	Chi and Kundalini Yoga	Multiscale fractal dimension	Kruskal-Wallis test	MSFD decreases ($p < 0.05$)
Goshvarpour And Goshvarpour [22]	Chi and Kundalini Yoga	lagged Poincare's plot	Wilcoxon rank sum test	As the delay increases, the symmetry of the HRV increased in pre Chi, on Chi, pre Yoga ($p < 0.05$)
Raghavendra and Dutt [55]	Chi and Kundalini Yoga	Nonlinear analysis using CD, LLE, minimum embedding dimension and nonlinearity score	Kruskal–Wallis test	MED and CD decrease; NLS and LLE increase ($p < 0.05$)
Peng et al. [37]	Chi and Kundalini Yoga	Time-frequency analysis using Hilbert transform and Lomb periodogram	Student's t-test	The amplitude of oscillations increase ($p < 0.01$)
Sarkar and Barat [56]	Chi and Kundalini Yoga	Nonlinear analysis using DFA, diffusion entropy analysis, recurrence quantification analysis, and multiscale entropy	Mann–Whitney U test	MSE at large scales increases ($p < 0.01$)
Our proposed method	Chi and Kundalini Yoga	GIC And PS based VG	ANOVA test	$p < 0.05$

conditions like meditation.

The authors believe that the new findings obtained in this study, as a result of evolution in practice, will play an important role in improving therapy. In the future, analyzing this method with other meditation techniques is needed to demonstrate further the reliability and potential power of our proposed method. Another future research direction could be combining VGs proposed in this study with other VG algorithms for scrutinizing changes in heart function during meditation techniques. The other important direction would be to examine deep learning architectures to elicit the latent dynamical features in HR time series. In addition, applying multi-scale entropy and multi-fractality to assess complexity and provide a benchmark in investigating cardiac states, such as meditation, could be an absorbing subject of future work.

Declaration of competing interest

The authors declare that they have no known competing financial interests or personal relationships that could have appeared to influence the work reported in this paper.

Data availability

Data will be made available on request.

References

[1] S.G. Hofmann, A.T. Sawyer, A.A. Witt, D. Oh, The effect of mindfulness-based therapy on anxiety and depression: a meta-analytic review, J. Consult. Clin. Psychol. 78 (2) (2010) 169.

[2] C.C. Streeter, P.L. Gerbarg, R.B. Saper, D.A. Ciraulo, R.P. Brown, Effects of yoga on the autonomic nervous system, gamma-aminobutyric-acid, and allostasis in epilepsy, depression, and post-traumatic stress disorder, Med. Hypotheses 78 (5) (2012) 571–579.

[3] S. Feruglio, A. Matiz, G. Pagnoni, F. Fabbro, C. Crescentini, The impact of mindfulness meditation on the wandering mind: a systematic review, Neurosci. Biobehav. Rev. 131 (2021) 313–330.

[4] Y.Y. Tang, Y. Ma, Y. Fan, H. Feng, J. Wang, S. Feng, M. Fan, Central and autonomic nervous system interaction is altered by short-term meditation, Proc. Natl. Acad. Sci. USA 106 (22) (2009) 8865–8870.

[5] R.K. Wallace, Physiological effects of transcendental meditation, Science 167 (3926) (1970) 1751–1754.

[6] S. Phongsuphap, Y. Pongsupap, P. Chandanamattha, C. Lursinsap, Changes in heart rate variability during concentration meditation, Int. J. Cardiol. 130 (3) (2008) 481–484.

[7] P.S. Nijjar, V.K. Puppala, O. Dickinson, S. Duval, D. Duprez, M.J. Kreitzer, D. G. Benditt, Modulation of the autonomic nervous system assessed through heart rate variability by a mindfulness based stress reduction program, Int. J. Cardiol. 177 (2) (2014) 557–559.

[8] C.A. Fernandes, Y.K. Nóbrega, C.E. Tosta, Pranic meditation affects phagocyte functions and hormonal levels of recent practitioners, J. Alternative Compl. Med. 18 (8) (2012) 761–768.

[9] R.P. Nagendra, N. Maruthai, B.M. Kutty, Meditation and its regulatory role on sleep, Front. Neurol. 3 (2012) 54.

[10] E.R. Kasala, L.N. Bodduluru, Y. Maneti, R. Thipparaboina, Effect of meditation on neurophysiological changes in stress mediated depression, Compl. Ther. Clin. Pract. 20 (1) (2014) 74–80.

[11] D. Deka, B. Deka, Characterization of heart rate variability signal for distinction of meditative and pre-meditative states, Biomed. Signal Process Control 66 (2021), 102414.

[12] S. Chatterjee, J.R. Chowdhury, A. Dey, How to realize the effect of Kundalini yoga and Chinese Chi meditation on the HRV and ANS with GAN architecture?'HRV-GAN': an alternative approach, Biomed. Signal Process Control 77 (2022), 103822.

[13] D. Deka, B. Deka, Detection of meditation-induced HRV dynamics using averaging technique-based oversampled feature set and machine learning classifiers, IEEE Access 11 (2023) 29576–29590.

[14] J. Alvarez-Ramirez, E. Rodríguez, J.C. Echeverría, Fractal scaling behavior of heart rate variability in response to meditation techniques, Chaos, Solit. Fractals 99 (2017) 57–62.

[15] J. Li, J. Hu, Y. Zhang, X. Zhang, Dynamical complexity changes during two forms of meditation, Phys. Stat. Mech. Appl. 390 (12) (2011) 2381–2387.

[16] N. Tian, H. Yu, S. Zhao, G. Liu, R. Song, Modified multiscale transfer entropy analysis of intra-and inter-couplings of cardio-respiratory systems during meditation, Biomed. Signal Process Control 79 (2023), 103983.

[17] A. Sarkar, P. Barat, Effect of meditation on scaling behavior and complexity of human heart rate variability, Fractals 16 (3) (2008) 199–208.

[18] E. Conte, A. Khrennikov, A. Federici, J.P. Zbilut, Fractal fluctuations and quantum-like chaos in the brain by analysis of variability of brain waves: a new method based on a fractal variance function and random matrix theory, Chaos, Solit. Fractals 41 (2009) 2790–2800.

[19] M. Nasrolahzadeh, J. Haddadnia, Analysis of mean square estimation surface and its corresponding contour plots of heart rate signals during meditation with adaptive wiener filter, in: 8th Middle East Cardiovascular Congress, 4–6 June 2014 Istanbul-Turkey, 2014.

[20] Y. Lu, J. Rodriguez-Larios, Nonlinear EEG signatures of mind wandering during breath focus meditation, Current Research in Neurobiology 3 (2022), 100056.

[21] A. Goshvarpour, A. Goshvarpour, Do meditators and non-meditators have different HRV dynamics? Cognit. Syst. Res. 54 (2019) 21–36, 1.

[22] A. Goshvarpour, A. Goshvarpour, Asymmetry of lagged Poincare plot in heart rate signals during meditation, Journal of traditional and complementary medicine 11 (1) (2021) 16–21.

[23] A. Goshvarpour, A. Goshvarpour, Matching pursuit based indices for examining physiological differences of meditators and non-meditators: an HRV study, Phys. Stat. Mech. Appl. 524 (2019) 147–156.

[24] A. Delorme, R. Grandchamp, J. Curot, G. Barragan-Jason, M. Denuelle, J.C. Sol, L. Valton, Effect of meditation on intracerebral EEG in a patient with temporal lobe epilepsy: a case report, Explore 17 (3) (2021) 197–202.

[25] T. Xue, B. Chiao, T. Xu, H. Li, K. Shi, Y. Cheng, D. Cui, The heart-brain axis: a proteomics study of meditation on the cardiovascular system of Tibetan Monks, EBioMedicine 80 (2022), 104026.

[26] H. Wahbeh, A. Sagher, W. Back, P. Pundhir, F. Travis, A systematic review of transcendent states across meditation and contemplative traditions, Explore 14 (1) (2018) 19–35.

[27] L. Lacasa, B. Luque, J. Luque, J.C. Nuno, The visibility graph: a new method for estimating the Hurst exponent of fractional Brownian motion, EPL (Europhysics Letters) 86 (3) (2009), 30001.

[28] A. Bhaduri, D. Ghosh, Quantitative assessment of heart rate dynamics during meditation: an ECG based study with multi-fractality and visibility graph, Front. Physiol. 7 (2016) 44.

[29] Z. Mohammadpoory, J. Haddadnia, M. Azizi, Epileptic seizure detection based on the Limited Penetrable visibility graph algorithm and graph properties, Iranian Journal of Medical Physics 15.Special Issue-12th, Iranian Congress of Medical Physics (2018) 286, 286.

[30] M. Mozaffarilegha, H. Adeli, Visibility graph analysis of speech evoked auditory brainstem response in persistent developmental stuttering, Neurosci. Lett. 696 (2019) 28–32.

[31] M. Ahmadlou, H. Adeli, Visibility graph similarity: a new measure of generalized synchronization in coupled dynamic systems, Phys. Nonlinear Phenom. 241 (4) (2012) 326–332.

[32] W. Li, H. Wang, L. Zhuang, S. Han, H. Zhang, J. Wang, Weighted multi-scale limited penetrable visibility graph for exploring atrial fibrillation rhythm, Signal Process. 189 (2021), 108288.

[33] Z. Mohammadpoory, M. Nasrolahzadeh, N. Mahmoodian, J. Haddadnia, Automatic identification of diabetic retinopathy stages by using fundus images and visibility graph method, Measurement 140 (2019) 133–141.

[34] Z. Mohammadpoory, M. Nasrolahzadeh, J. Haddadnia, Epileptic seizure detection in EEG signals based on the weighted visibility graph entropy, Seizure: European journal of epilepsy 50 (2017) 202–208.

[35] M. Nasrolahzadeh, Z. Mohammadpoory, J. Haddadnia, Analysis of heart rate signals during meditation using visibility graph complexity, Cognitive neurodynamics 13 (1) (2019) 45–52.

[36] Z. Mohammadpoory, M. Nasrolahzadeh, N. Mahmoodian, M. Sayyah, J. Haddadnia, Complex network based models of ecog signals for detection of induced epileptic seizures in rats, Cognitive neurodynamics 13 (4) (2019) 325–339.

[37] C.K. Peng, J.E. Mietus, Y. Liu, G. Khalsa, P.S. Douglas, H. Benson, A.L. Goldberger, Exaggerated heart rate oscillations during two meditation techniques, Int. J. Cardiol. 70 (1999) 101–107.

[38] A. Le Guennec, S. Malinowski, R. Tavenard, September). Data augmentation for time series classification using convolutional neural networks, in: ECML/PKDD Workshop on Advanced Analytics and Learning on Temporal Data, 2016.

[39] L. Lacasa, B. Luque, F. Ballesteros, J. Luque, J.C. Nuno, From time series to complex networks: the visibility graph, Proc. Natl. Acad. Sci. USA 105 (13) (2008) 4972–4975.

[40] S. Supriya, S. Siuly, H. Wang, J. Cao, Y. Zhang, Weighted visibility graph with complex network features in the detection of epilepsy, IEEE Access 4 (2016) 6554–6566.

[41] M. Ahmadlou, H. Adeli, A. Adeli, New diagnostic EEG markers of the Alzheimer's disease using visibility graph, J. Neural. Transm. 117 (9) (2010) 1099–1109.

[42] J. Kim, T. Wilhelm, What is a complex graph? Phys. Stat. Mech. Appl. 387 (11) (2008) 2637–2652.

[43] M. Ahmadlou, H. Adeli, Complexity of weighted graph: a new technique to investigate structural complexity of brain activities with applications to aging and autism, Neurosci. Lett. 650 (2017) 103–108.

[44] M. Nasrolahzadeh, A. Ibrahim, S. Rahnamayan, J. Haddadnia, Pareto-radvis: a novel visualization scheme for many-objective optimization, in: 2020 IEEE International Conference on Systems, , Man, and Cybernetics (SMC), 2020, pp. 3868–3873.

[45] Y. Karaca, Multi-chaos, fractal and multi-fractional AI in different complex systems, in: Multi-Chaos, Fractal and Multi-Fractional Artificial Intelligence of Different Complex Systems, 2022, pp. 21–54.

[46] P. Castiglioni, D. Lazzeroni, P. Coruzzi, A. Faini, Multifractal-multiscale analysis of cardiovascular signals: a DFA-based characterization of blood pressure and heart-rate complexity by gender, Complexity 2018 (2018).

[47] A. Richard, P. Orio, E. Tanré, An integrate-and-fire model to generate spike trains with long-range dependence, J. Comput. Neurosci. 44 (3) (2018) 297–312.
[48] H. Adeli, S. Ghosh-Dastidar, N. Dadmehr, A wavelet-chaos methodology for analysis of EEGs and EEG subbands to detect seizure and epilepsy, IEEE Transactions on Biomedical Engineering 54 (2) (2007) 205–211.
[49] A. Bhaduri, S. Bhaduri, D. Ghosh, Visibility graph analysis of heart rate time series and bio-marker of congestive heart failure, Phys. Stat. Mech. Appl. 482 (2017) 786–795.
[50] M.C. Pascoe, M. de Manincor, J. Tseberja, M. Hallgren, P.A. Baldwin, A.G. Parker, Psychobiological mechanisms underlying the mood benefits of meditation: a narrative review, Comprehensive Psychoneuroendocrinology 6 (2021), 100037.
[51] F. Travis, L. Valosek, A. Konrad IV, J. Link, J. Salerno, R. Scheller, S. Nidich, Effect of meditation on psychological distress and brain functioning: a randomized controlled study, Brain Cognit. 125 (2018) 100–105.
[52] S.S. Khalsa, D. Rudrauf, R.J. Davidson, D. Tranel, The effect of meditation on regulation of internal body states, Front. Psychol. 6 (2015) 924.
[53] P. Zeng, H. Liu, H. Ni, J. Zhou, L. Xia, X. Ning, Multiscale power analysis for heart rate variability, AIP Adv. 5 (6) (2015), 067164.
[54] B.S. Raghavendra, D.N. Dutt, Multiscale fractal dimension technique for characterization and analysis of biomedical signals, in: 2011 Digital Signal Processing and Signal Processing Education Meeting, DSP/SPE), 2011, pp. 370–374.
[55] B.S. Raghavendra, D.N. Dutt, Nonlinear dynamical characterization of heart rate variability time series of meditation, Health (Irvine. Calif) 3 (2010) 10.
[56] A. Sarkar, P. Barat, Effect of meditation on scaling behavior and complexity of human heart rate variability, Fractals 16 (3) (2008) 199–208.